On the Effect of Initial Curvature on Cracked Flat Sheets

E. S. FOLIAS

College of Engineering, University of Utah, Salt Lake City, U.S.A.

(Received January 24, 1969)

ABSTRACT
A survey of existing solutions describing the stress distribution around the crack tip of an initially curved sheet is made
and a method for estimating approximate stress intensity factors of other more complicated shell geometries is dis-
cussed.

Notation

$A_s^{(e)}, A_{c,a}^{(e)}, A_s^{(b)}, A_{c,a}^{(b)}$ $a_s^{(e)}, a_{c,a}^{(e)}, a_s^{(b)}, a_{c,a}^{(b)}$	$=$ as defined in text
c	$=$ half crack length
$D \equiv Eh^3/[12(1-v^2)]$	$=$ flexural rigidity
E	$=$ Young's modulus
$F(x, y)$	$=$ stress function
G	$=$ shear modulus
h	$=$ thickness
L	$=$ linear dimension
$P_s^{(e)}, P_p^{(e)}, P_{c,a}^{(e)}, P_{c,c}^{(e)}, P_{c,a}^{(e)}$ $P_s^{(b)}, P_p^{(b)}, P_{c,a}^{(e)}, P_{c,c}^{(e)}, P_{c,a}^{(e)}$	$=$ stress coefficients as defined in text
$q(x, y)$	$=$ internal pressure
q_0	$=$ uniform internal pressure
R, R_x, R_y, R_1, R_2	$=$ radii of an initially curved sheet
$R = (x^2+y^2)^{\frac{1}{2}}, \theta = \tan^{-1}(y/x)$	
$w(x, y)$	$=$ displacement function
$w_0(x, y)$	$=$ initial displacement function
x, y, z	$=$ rectangular cartesian coordinates
α	$=$ orientation angle as defined in Fig. 17
γ	$= 0.5768\ldots =$ Euler's constant
ε	$=$ as defined in Fig. 18
λ^4	$\equiv \dfrac{Ehc^4}{R^2 D} \equiv \dfrac{12(1-v^2)c^4}{R^2 h^2}$
$\lambda_1, \lambda_2, \lambda_3, \lambda_x, \lambda_y$	$\equiv$ as defined in text
v	$=$ Poisson's ratio
v_0	$\equiv 1-v$
π	$= 3.14$
σ_h	$=$ hoop stress
σ_n	$=$ just ahead normal to the crack prolongation stress
$\sigma_x^{(e)}, \sigma_y^{(e)}, \tau_{xy}^{(e)}$	$=$ stretching stress components
$\sigma_x^{(b)}, \sigma_y^{(b)}, \tau_{xy}^{(b)}$	$=$ bending stress components
$\bar{\sigma}^{(e)}$	$=$ applied stretching stress
$\bar{\sigma}^{(b)}$	$=$ applied bending stress
$\bar{\tau}^{(e)}$	$=$ applied in-plane shear
$\bar{\tau}^{(b)}$	$=$ applied equivalent shear

Introduction

One of the problems in fracture mechanics relating to the design of monocoque structures and pressure vessels deals with the stresses in the neighborhood of a crack in an initially curved sheet. The inherent consequences of initial curvature are the presence of an interaction between bending and stretching and the presence of higher stress levels than those found in a similarly loaded flat plate. Thus initially curved panels present a reduced resistance to fracture initiation that is basically of geometric origin.

The author, in this paper, reviews some of his previous work on initially curved sheets and discusses further extensions of his work to cover other more general shell geometries.

General Theory

In the following, we consider bending and stretching of thin shallow* shells, as described by traditional two-dimensional linear theory. In speaking of the formulation of two-dimensional differential equations, we mean the transition from the exact three-dimensional elasticity problem to that of two-dimensional approximate formulation, which is appropriate in view of the "thinness" of the shell. We will, furthermore, limit ourselves to elastic, isotropic, homogeneous and constant thickness, shallow segments of shells, subjected to small deformations and strains.

The basic variables in the theory of shallow shells are the displacement comment $w(x, y)$ in the direction of an axis z and a stress function $F(x, y)$ which represents the stress resultants tangent to the middle surface of the shell. Following Marguerre [2], the coupled differential
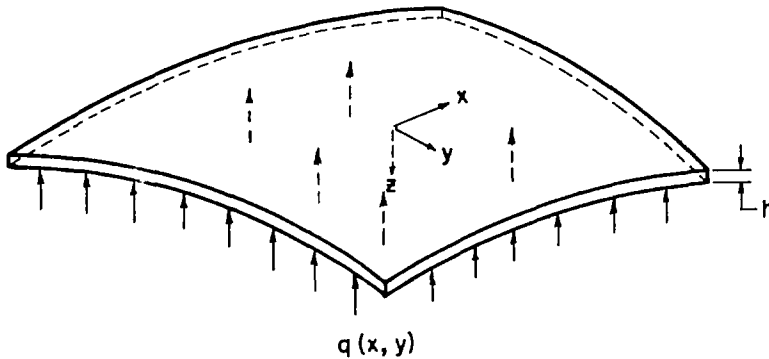

q (x, y)

Figure 1. Initially curved sheet.

equations governing w and F, with x and y as rectangular cartesian coordinates of the base plane (see Fig. 1), are given by:

$$\nabla^4 F = Eh \left[2 \frac{\partial^2 w_0}{\partial x\, \partial y} \frac{\partial^2 w}{\partial x\, \partial y} - \frac{\partial^2 w_0}{\partial x^2} \frac{\partial^2 w}{\partial y^2} - \frac{\partial^2 w_0}{\partial y^2} \frac{\partial^2 w}{\partial x^2} \right] \tag{1}$$

$$D\nabla^4 w = -q - 2 \frac{\partial^2 F}{\partial x\, \partial y} \frac{\partial^2 w_0}{\partial x\, \partial y} + \frac{\partial^2 F}{\partial x^2} \frac{\partial^2 w_0}{\partial y^2} + \frac{\partial^2 F}{\partial y^2} \frac{\partial^2 w_0}{\partial x^2}, \tag{2}$$

where $w_0(x, y)$ describes the initial shape of the shell in reference to that of a flat plate.

Formulation of the General Problem

Let us consider a portion of a thin, shallow shell, of constant thickness h, subjected to an internal pressure $q(x, y)$ and containing a crack of length $2c$ (see Fig. 2). Our problem therefore,

* According to Ogibalov [1], a shell will be called. shallow if the least radius of curvature is greater by one order of magnitude than the linear dimensions, i.e. $L/R \leq 0.1$; and thin if $h/R \leq 0.01$.

is to find two functions $F(x, y)$ and $w(x, y)$ such that they satisfy the governing differential equations (1) and (2), and the appropriate boundary conditions. That is, we require that: (i) on the faces of the crack, the normal moment, equivalent shear, and normal and tangential membrane forces vanish, and (ii) away from the crack, the appropriate loading and support conditions are satisfied.
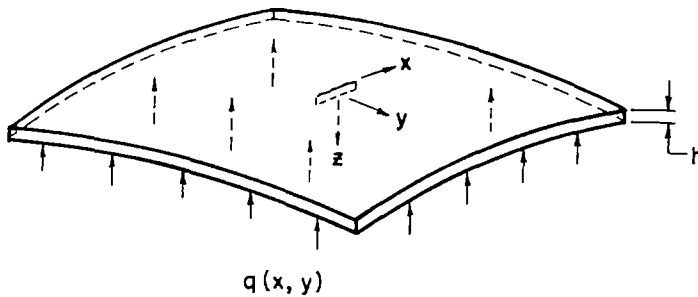

Figure 2. Initially curved sheet containing a finite line crack

In treating this problem, it is found convenient to seek the solution into two parts, the "undisturbed" or "particular" solution which satisfies equations (1) and (2) and the loading and support conditions but leaves residual forces along the crack*, and the "complementary" solution which precisely nullifies these residuals and offers no contribution far from the crack.

It is evident from the applicable differential equations that a theoretical attack of the general problem for an arbitrary initial curvature presents formidable mathematical complexities. However for the two simple geometries, spherical and cylindrical, exact solutions have been obtained in an asymptotic form. On the other hand, for other more complicated shell geometries the results can be obtained by a proper superposition of the two previous solutions.

1. Spherical shell

For a shallow spherical shell the radius of curvature remains constant in all directions therefore,

$$\frac{\partial^2 w_0}{\partial x \, \partial y} = 0 \; ; \quad \frac{\partial^2 w_0}{\partial x^2} = \frac{\partial^2 w_0}{\partial y^2} = \frac{1}{R} \, . \tag{3a}$$

Substituting (3a) into (1) and (2) one recovers Reissner's equations, *i.e.*

$$\frac{Eh}{R} \nabla^2 w + \nabla^4 F = 0 \tag{1a}$$

$$\nabla^4 w - \frac{1}{RD} \nabla^2 F = -\frac{q}{D} \, . \tag{2a}$$

For a spherical cap containing at the apex a finite crack of length $2c$ (see Fig. 3) the author [3], using an integral formulation, reduced the problem to the solution of two coupled singular integral equations. The solution to those was sought in a power series of λ, where λ was given by

$$\lambda \equiv \left(\frac{Ehc^4}{R^2 D}\right)^{\frac{1}{4}} \equiv \{12(1-v^2)\}^{\frac{1}{4}} \{(R/h)\}^{\frac{1}{2}} \frac{c}{R} \equiv \{12(1-v^2)\}^{\frac{1}{4}} \frac{c}{(Rh)^{\frac{1}{2}}} \, . \tag{4}$$

Furthermore, the author has shown [3b] that for λ less than a calculated bound the series solution does converge to the exact.

It is clear from equation (4) that λ is small for large ratios of R/h and small crack lengths. As a practical matter, if one considers crack lengths less than one tenth of the periphery, *i.e.*
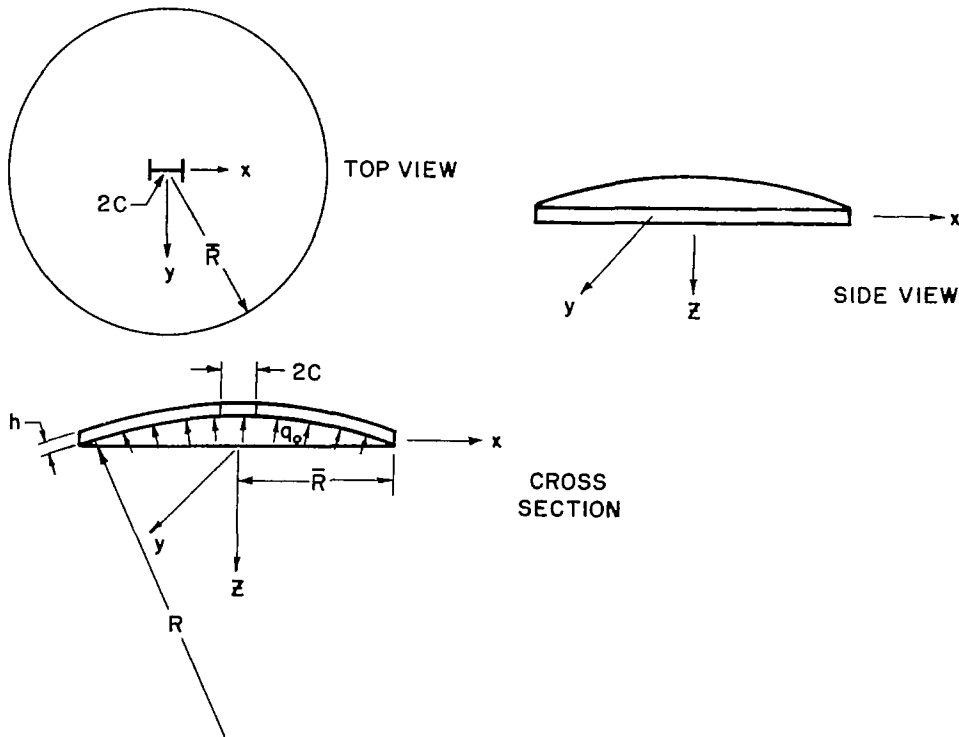
* For more details, see [3].

Figure 3. Geometrical configurations of a pressurized spherical cap.

$2c < (2\pi R/10)$, and for $(R/h) < 10^3$ a corresponding upper bound for λ can be obtained, i.e. $\lambda < 20$. Thus the range of λ becomes $0 < \lambda < 20$ and for most practical cases is between 0 and 3, depending upon the size of the crack. Consequently, an asymptotic expansion for small λ is justifiable.

Without getting into the details, the stress distribution around the crack tip for a symmetrical loading[*] is:

Extensional stresses: through the thickness

$$\sigma_x^{(e)} = P_s^{(e)} (c/2r)^{\frac{1}{2}} \left(\frac{3}{4} \cos \frac{\theta}{2} + \frac{1}{4} \cos \frac{5\theta}{2} \right) + O(r^0) \tag{5}$$

$$\sigma_y^{(e)} = P_s^{(e)} (c/2r)^{\frac{1}{2}} \left(\frac{5}{4} \cos \frac{\theta}{2} - \frac{1}{4} \cos \frac{5\theta}{2} \right) + O(r^0) \tag{6}$$

$$\tau_{xy}^{(e)} = P_s^{(e)} (c/2r)^{\frac{1}{2}} \left(-\frac{1}{4} \sin \frac{\theta}{2} + \frac{1}{4} \sin \frac{5\theta}{2} \right) + O(r^0) \tag{7}$$

Bending stresses: on the "tension side" of the shell

$$\sigma_x^{(b)} = P_s^{(b)} (c/2r)^{\frac{1}{2}} \left(-\frac{3-3v}{4} \cos \frac{\theta}{2} - \frac{1-v}{4} \cos \frac{5\theta}{2} \right) + O(r^0) \tag{8}$$

$$\sigma_y^{(b)} = P_s^{(b)} (c/2r)^{\frac{1}{2}} \left(\frac{11+5v}{4} \cos \frac{\theta}{2} + \frac{1-v}{4} \cos \frac{5\theta}{2} \right) + O(r^0) \tag{9}$$

$$\tau_{xy}^{(b)} = P_s^{(b)} (c/2r)^{\frac{1}{2}} \left(-\frac{7+v}{4} \sin \frac{\theta}{2} - \frac{1-v}{4} \sin \frac{5\theta}{2} \right) + O(r^0) \tag{10}$$

[*] For antisymmetric loadings, see reference 3b.

where

$$P_s^{(e)} = \bar{\sigma}^{(e)} \left\{ 1 + \frac{3\pi}{32} \lambda^2 \right\} + \bar{\sigma}^{(b)} \frac{(\lambda^2)(1-v^2)^{\frac{1}{2}}}{3^{\frac{1}{2}}(4-v_0)} \left\{ \frac{7}{32} + \frac{3}{8} \left(\gamma + \ln \frac{\lambda}{4} \right) \right\} + O(\lambda^4 \ln \lambda) \qquad (11a)$$

and

$$P_s^{(b)} = -\bar{\sigma}^{(e)} \frac{\lambda^2 (3^{\frac{1}{2}})}{(1-v^2)^{\frac{1}{2}}(4-v_0)} \left\{ \frac{8-7v_0}{32} + \frac{4-3v_0}{8} \left(\gamma + \ln \frac{\lambda}{4} \right) \right\} +$$
$$- \frac{\bar{\sigma}^{(b)}}{4-v_0} \left\{ 1 + \frac{4-3v_0}{4-v_0} \frac{\pi\lambda^2}{32} \right\} + O(\lambda^4 \ln \lambda) \qquad (12a)$$

It should be emphasized that the stress coefficients contain only up to $O(\lambda^2)$ terms hence, their use is limited to small values of the parameter λ, in particular $\lambda < 1$. If one, however, wishes to know the stress coefficients for large values of λ, it is necessary to consider higher order terms in order to guarantee convergence. This matter was investigated further by Erdogan and Kibler [4] who, by the aid of a computer, were able to extend the results of reference [3] to include values of $\lambda \leq 5.5$. Thus, for Poisson's ratio of $\frac{1}{3}$, an alternate form of the stress coefficients good up to $\lambda \leq 5.5$ is:

$$P_s^{(e)} = \bar{\sigma}^{(e)} A_s^{(e)} - 0.54\bar{\sigma}^{(b)} a_s^{(e)} \qquad (13a)$$

$$P_s^{(b)} = 1.81\bar{\sigma}^{(e)} a_s^{(b)} - 0.30\bar{\sigma}^{(b)} A_s^{(b)} , \qquad (14a)$$

where the coefficients $A_s^{(e)}$, $A_s^{(b)}$, $a_s^{(e)}$ and $a_s^{(b)}$ are functions of λ and are given in Table 1 or by Figures 4–7.

TABLE 1

Sphere

λ	$A_s^{(e)}$	$A_s^{(b)}$	$a_s^{(e)}$	$a_s^{(b)}$
0.2	1.0112	1.0020	0.00842	0.00611
0.4	1.0422	1.0070	0.02249	0.01693
0.6	1.0887	1.0137	0.03749	0.02919
0.8	1.1479	1.0211	0.05202	0.04186
1.0	1.2174	1.0287	0.06557	0.05448
1.2	1.2956	1.0364	0.07799	0.06685
1.4	1.3812	1.0439	0.08935	0.07886
1.6	1.4731	1.0512	0.09964	0.09045
1.8	1.5706	1.0583	0.10895	0.10155
2.0	1.6729	1.0652	0.11740	0.11216
2.2	1.7795	1.0718	0.12519	0.12223
2.4	1.8899	1.0783	0.13228	0.13172
2.6	2.0038	1.0845	0.13876	0.14058
2.8	2.1208	1.0905	0.14475	0.14879
3.0	2.2408	1.0964	0.15030	0.15630
3.25	2.3947	1.1035	0.15668	0.16463
3.50	2.5526	1.1103	0.16260	0.17172
3.75	2.7143	1.1170	0.1681	0.17751
4.00	2.8796	1.1233	0.1732	0.18194
4.25	3.0485	1.1297	0.1780	0.18483
4.50	3.2208	1.1357	0.1826	0.18644
5.00	3.5750	1.1470	0.1905	0.18493
5.50	3.9446	1.1580	0.2000	0.17802

2. *Flat plate*

The flat plate represents the degenerative case of a spherical cap where the radius now is infinite therefore,
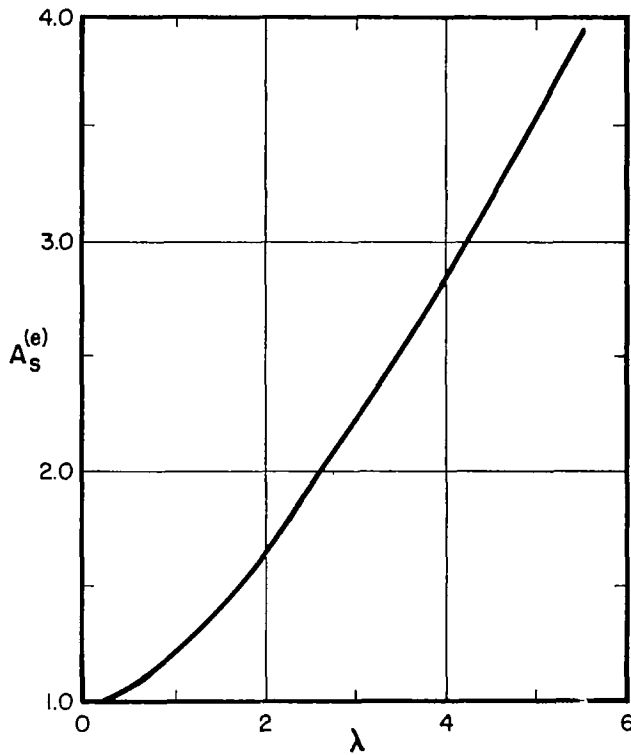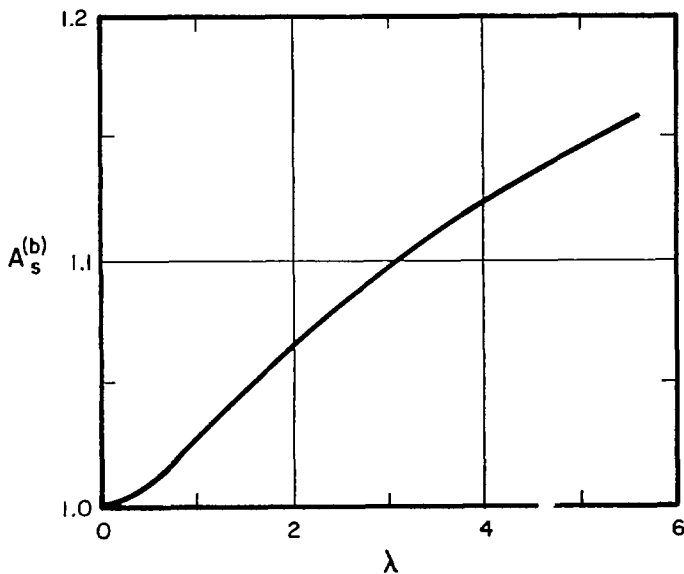
Figure 4. Stress coefficient for a sphere [4].

Figure 5. Stress coefficient for a sphere [4].

$$\frac{\partial^2 w_0}{\partial x \, \partial y} = \frac{\partial^2 w_0}{\partial x^2} = \frac{\partial^2 w_0}{\partial y^2} = 0 \ . \tag{3b}$$

Substituting (3b) into (1) and (2) one recovers the classical equations for a flat plate, *i.e.*

$$\nabla^4 F = 0 \tag{1b}$$

$$\nabla^4 w = -q/D \ . \tag{2b}$$

The problem of a flat plate containing a finite crack (see Fig. 8) has been investigated by
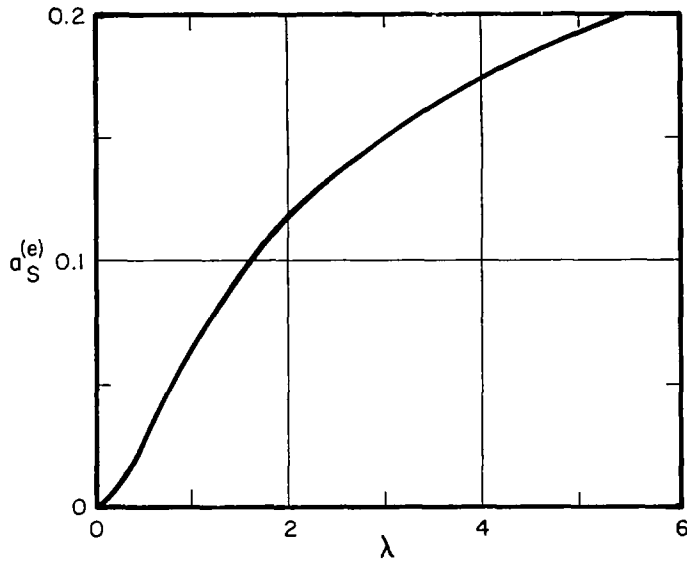
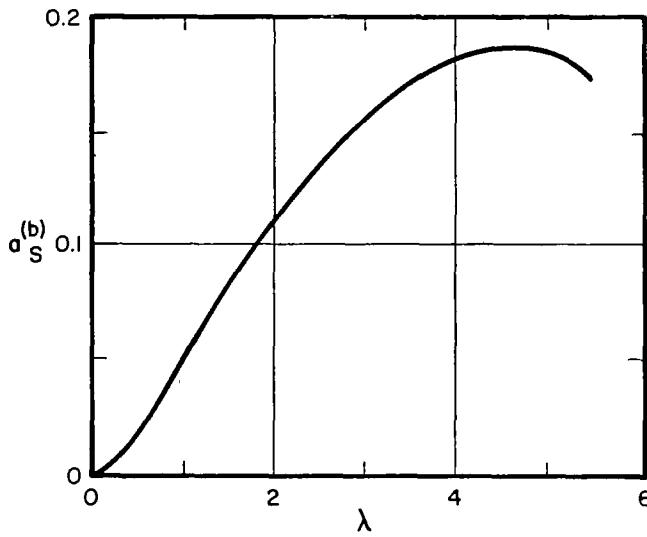Figure 6. Stress coefficient for a sphere [4].
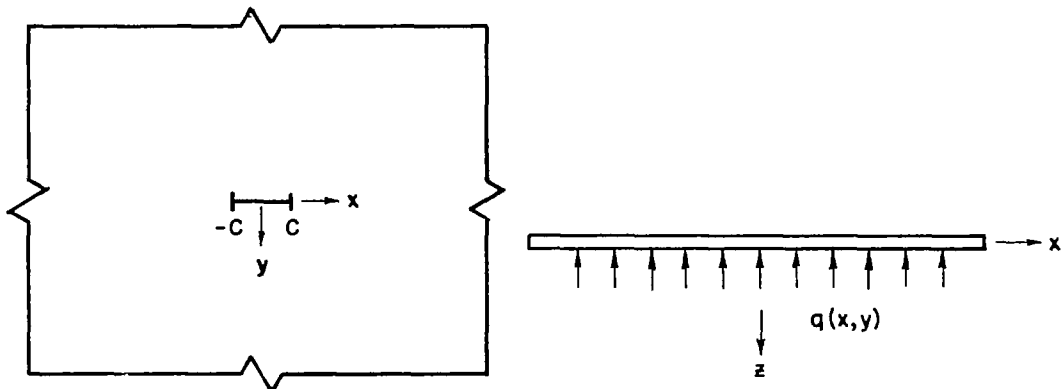

Figure 7. Stress coefficient for a sphere [4]

Figure 8. Cracked plate subjected to a lateral load q.

many authors for various types of loadings. The solution, however, can also be obtained from that of the spherical cap by letting $R \to \infty$ or $\lambda \to 0$. Thus the stresses around the crack tip are given precisely by equations (5)–(10) where the stress coefficients now are:

$$P_p^{(e)} = \bar{\sigma}^{(e)} \tag{11b}$$

$$P_p^{(b)} = -\frac{\bar{\sigma}^{(b)}}{4-v_0} . \tag{12b}$$

3. *Cylindrical vessel*

For a shallow cylindrical shell, one of the principal radii of curvatures is infinite while the other constant therefore,

$$\frac{\partial^2 w_0}{\partial x \, \partial y} = \frac{\partial^2 w_0}{\partial x^2} = 0 \; ; \quad \frac{\partial^2 w_0}{\partial y^2} = \frac{1}{R} . \tag{3c}$$

Substituting (3c) into (1) and (2) one recovers the equations for a shallow cylindrical shell, *i.e.*

$$\frac{Eh}{R} \frac{\partial^2 w}{\partial x^2} + \nabla^4 F = 0 \tag{1c}$$

$$\nabla^4 w - \frac{1}{RD} \frac{\partial^2 F}{\partial x^2} = -\frac{q}{D} . \tag{2c}$$
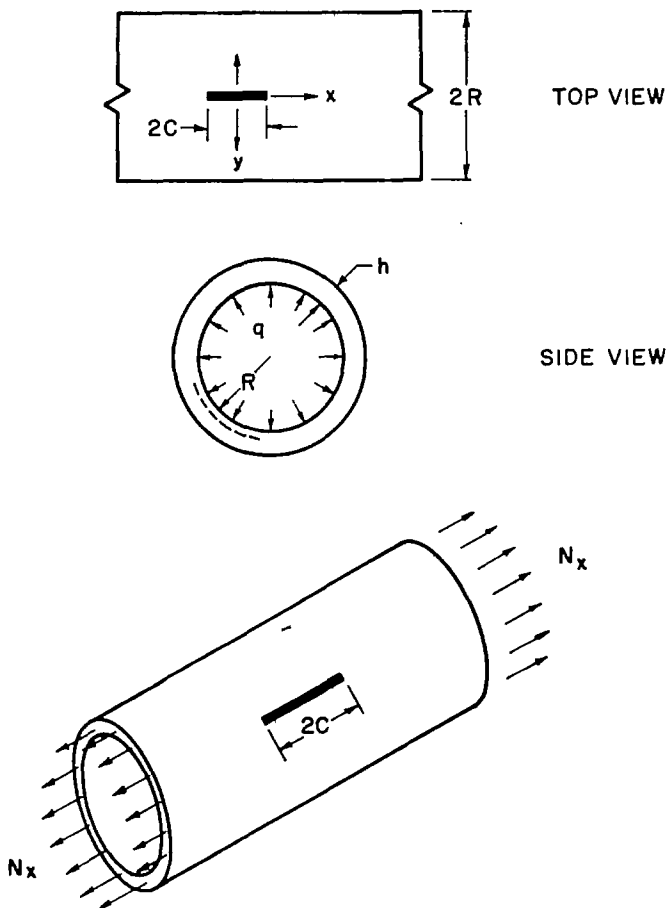

Figure 9. Geometry and coordinates of an axially cracked cylindrical shell under uniform axial extension N_x and internal pressure q_0.

Two cases of special interest immediately come to mind: an axial and a peripheral crack. Due to the mathematical complexities of this problem, Sechler and Williams [5] suggested an approximate method of solution, based upon the behavior of a beam on an elastic foundation and hence were able to obtain a reasonable agreement with the experimental results. The author, however, using the same method of solution as in reference [3] was able to investigate this problem in a more sophisticated manner and the details for an axial and a peripheral crack (see Figs. 9 and 10) can be found in references [6] and [7] respectively.

Subsequently, there have been two more theoretical analyses of this problem, the axial crack by Copley [8] and the peripheral crack by Duncan [9]. Their method of solution consists of the application of the Fourier Integral theorem leading to the derivation of two coupled singular integral equations (different in form than the author's) which in turn are approximated to high accuracy by matrix equations and are solved by the use of a computer. Their results were derived for zero "applied bending load," *i.e.* $\bar{\sigma}^{(b)} = 0$, and for Poisson's ratio $v = 0.32$.

Again omitting the mathematical details (see references [6] and [7]), the stresses around the crack tip are given also by equations (5)–(10) where the stress coefficients now are:

(i) for an axial crack

$$P_{c,a}^{(e)} = \bar{\sigma}^{(e)} \left\{ 1 + \frac{5\pi\lambda^2}{64} \right\} + \bar{\sigma}^{(b)} \frac{\lambda^2(1-v^2)^{\frac{1}{2}}}{3^{\frac{1}{2}}(4-v_0)} \left\{ \frac{42-37v_0}{96v_0} + \frac{6-5v_0}{16v_0} \cdot \left(\gamma + \ln \frac{\lambda}{8} \right) \right\} + O(\lambda^4 \ln \lambda);$$
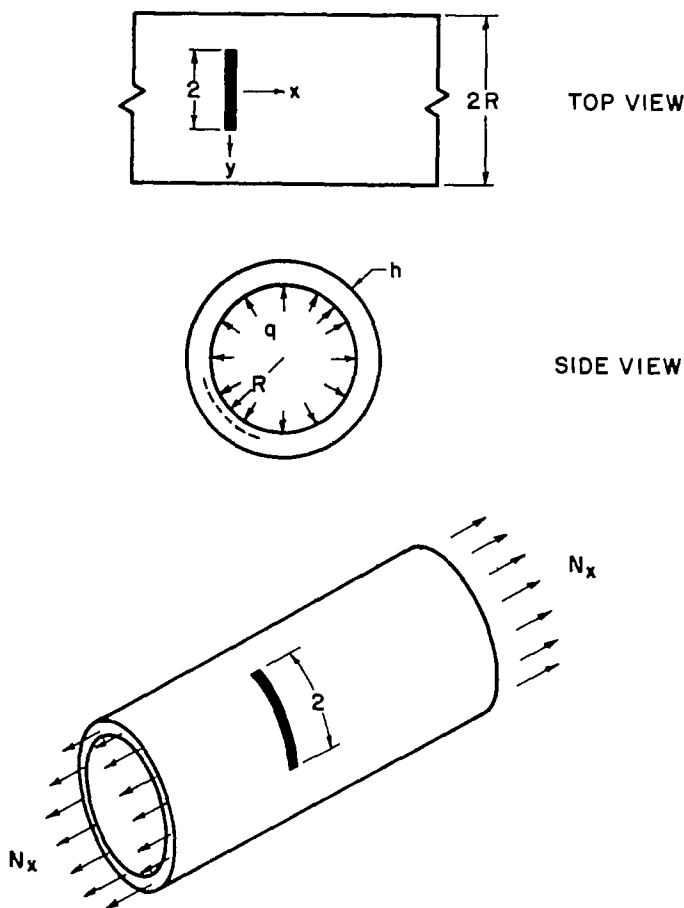
$$\lambda < 1 \qquad (11c)$$

Figure 10. Geometry and coordinates of a peripherally cracked cylindrical shell under uniform axial extension N_x and internal pressure q_0.
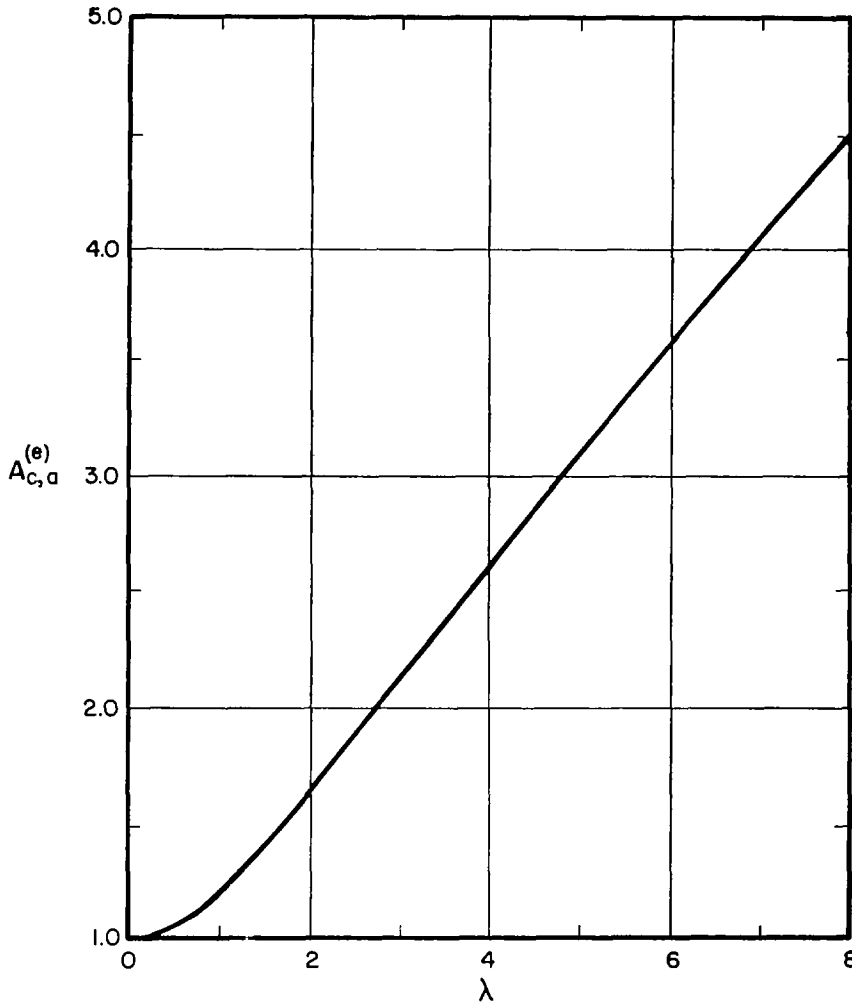
Figure 11. Stress coefficient for a cylinder [4].

$$P_{c,a}^{(b)} = -\bar{\sigma}^{(e)} \frac{\lambda^2(3^{\frac{1}{2}})}{(1-v^2)^{\frac{1}{2}}(4-v_0)} \left\{ \frac{42-37v_0}{96} + \frac{6-5v_0}{16}\left(\gamma + \ln\frac{\lambda}{8}\right) \right\}$$

$$- \frac{\bar{\sigma}^{(b)}}{4-v_0} \left\{ 1 + \frac{12v_0 - 5v_0^2 - 8}{(4-v_0)v_0} \frac{\pi\lambda^2}{64} \right\} + O(\lambda^4 \ln\lambda); \qquad\qquad \lambda < 1 \qquad (12\text{c})$$

or the alternate numerical form [4] valid for $v = \frac{1}{3}$ and $\lambda \leq 8$

$$P_{c,a}^{(e)} = \bar{\sigma}^{(e)} A_{c,a}^{(e)} - 0.54\bar{\sigma}^{(b)} a_{c,a}^{(e)} \qquad\qquad\qquad\qquad (13\text{c})$$

$$P_{c,a}^{(b)} = 1.81\bar{\sigma}^{(e)} a_{c,a}^{(b)} - 0.30\bar{\sigma}^{(b)} A_{c,a}^{(b)} . \qquad\qquad\qquad (14\text{c})$$

Here again the coefficients $A_{c,a}^{(e)}$, $A_{c,a}^{(b)}$, $a_{c,a}^{(e)}$ and $a_{c,a}^{(b)}$ are functions of λ and are given in Table 2 or by Figs. 11–14. In Fig. 15 we compare, for $\bar{\sigma}^{(b)} = 0$, the results of reference [4] with those of Copley's [8]. The comparison is very good up to $\lambda < 3.3$, beyond which Copley's results become somewhat higher.

(ii) *for a peripheral crack*

$$P_{c,p}^{(e)} = \bar{\sigma}^{(e)}\left\{ 1 + \frac{\pi\lambda^2}{64} \right\} + \bar{\sigma}^{(b)}\frac{\lambda^2(1-v^2)^{\frac{1}{2}}}{3^{\frac{1}{2}}(4-v_0)}\left\{ \frac{(1+v)}{32v_0} + \frac{(1+v)}{16v_0}\left(\gamma + \ln\frac{\lambda}{8}\right) \right\} + O(\lambda^4 \ln\lambda);$$

$$\lambda < 2.5 \qquad (11\text{d})$$

TABLE 2

Cylinder

| λ	$A_{c,a}^{(e)}$	$A_{c,a}^{(b)}$	$a_{c,a}^{(e)}$	$a_{c,a}^{(b)}$
0.2	1.0096	0.99816	0.006161	0.00410
0.4	1.0371	0.99340	0.01695	0.01124
0.6	1.0795	0.98660	0.02897	0 01902
0.8	1.1344	0.97846	0.04107	0.02659
1.0	1.1993	0.96946	0.05283	0.03359
1.2	1.2723	0.95986	0.06406	0.03985
1.4	1.3519	0.94993	0.07473	0.04529
1.6	1.4367	0.93976	0.08482	0.04990
1.8	1.5256	0.92956	0.09435	0.05368
2.0	1.6177	0.91936	0.1033	0.05664
2.2	1.7122	0.90923	0.1118	0.05883
2.4	1.8085	0.89926	0.1198	0.06018
2.6	1.9060	0.88940	0.1273	0.06090
2.8	2.0045	0.87970	0.1344	0.06083
3.0	2.1035	0.87023	0.1410	0.06014
3.25	2.2276	0.85863	0.1488	0.05832
3.50	2.3519	0.84740	0.1551	0.05549
3.75	2.4761	0.83643	0.1628	0.05172
4.00	2.5999	0.82440	0.1691	0.04700
4.25	2.7232	0.81542	0.1750	0.04154
4.50	2.8459	0.80539	0.1803	0.03512
5.00	3.0895	0.78616	0.1903	0.02012
5.50	3.3303	0.76832	0.2005	0.00234
6.00	3.5681	0.75079	0.2068	0.02222
6.50	3.8029	0.73446	0.2137	0.04130
7.00	4.0347	0.71879	0.2200	0.06622
7.50	4.2637	0.7080	0 2255	0.09350
8.00	4.4895	0.6897	0.2306	0.12279
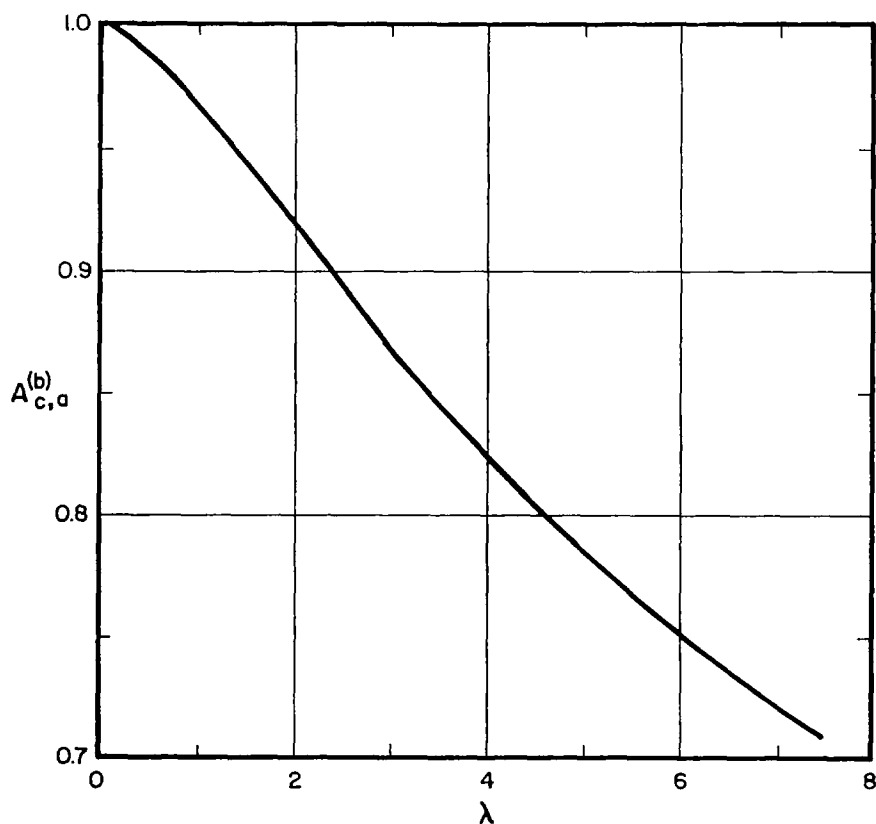
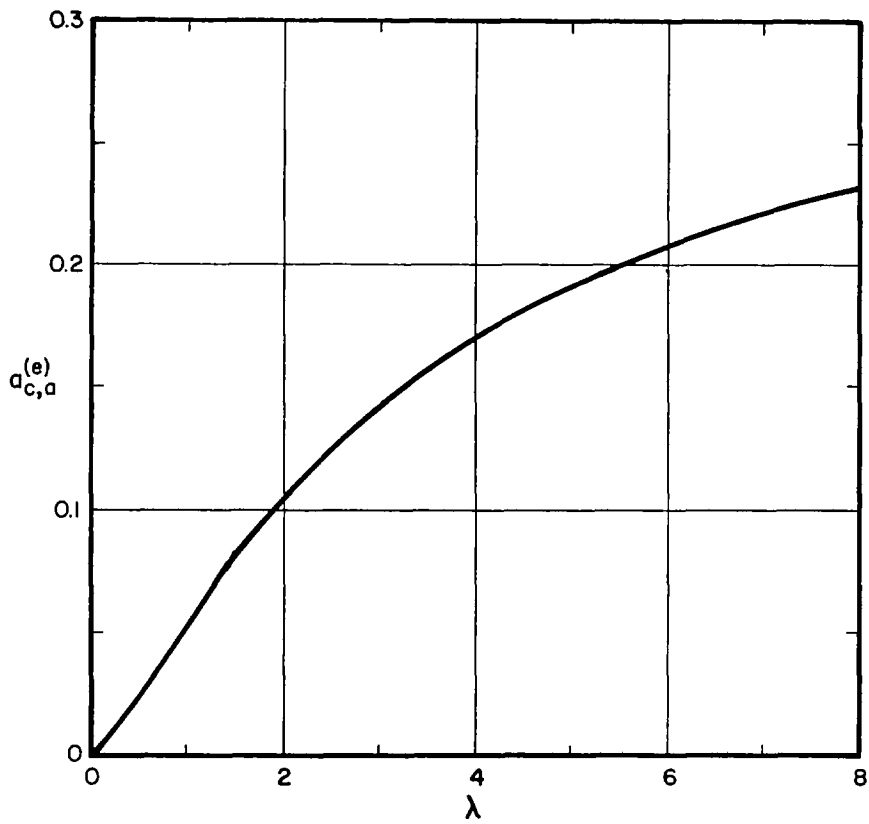Figure 12. Stress coefficient for a cylinder [4].
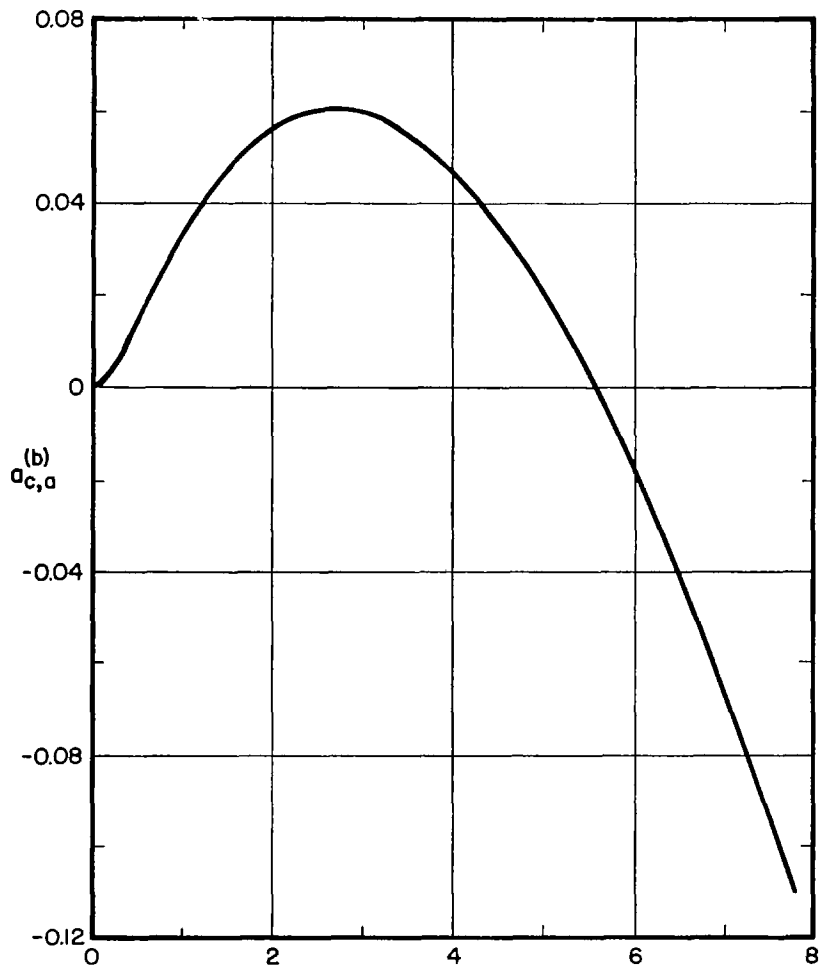
Figure 13. Stress coefficient for a cylinder [4].

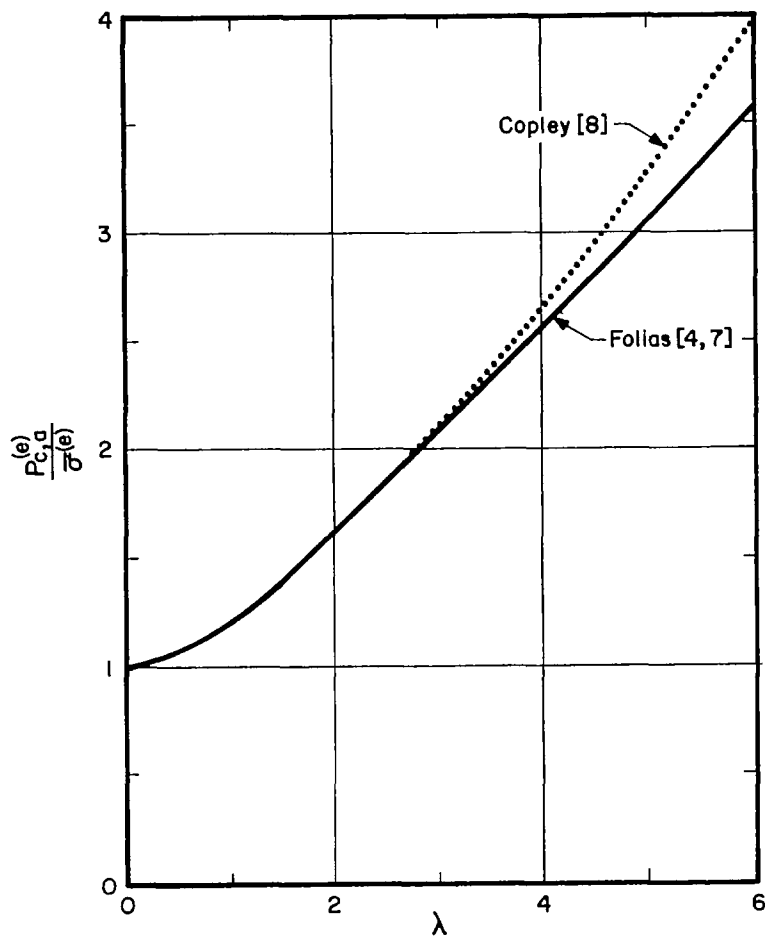Figure 14. Stress coefficient for a cylinder [4].

Figure 15. Comparison of the two methods for the stress coefficient of a cylindrical shell containing an axial crack.
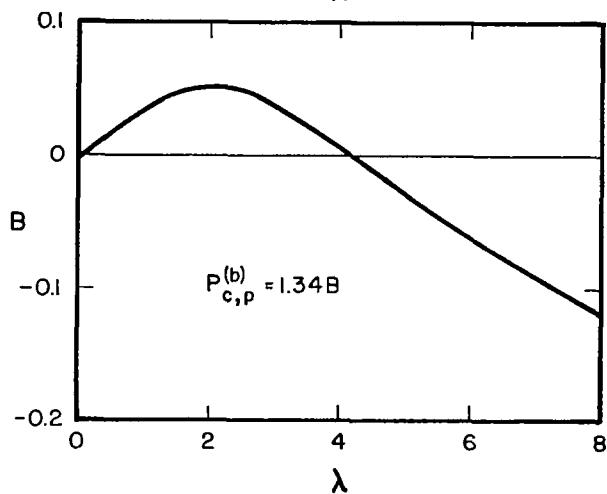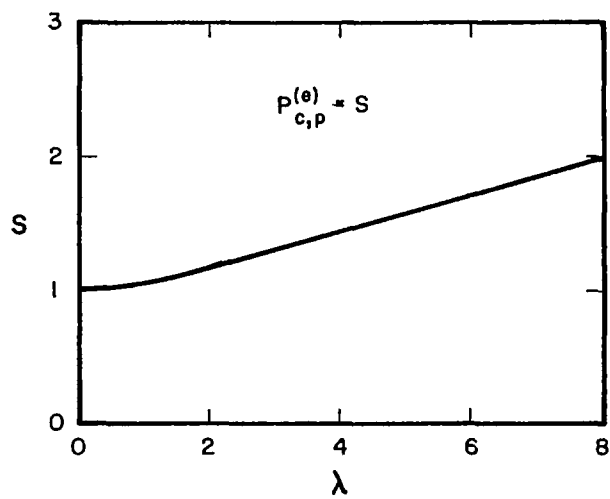

Figure 16. Duncan's stress coefficients for a cylindrical shell containing a peripheral crack.

$$P_{c,p}^{(b)} = -\bar{\sigma}^{(e)} \frac{\lambda^2 (3^{\frac{1}{4}})}{(1-v^2)^{\frac{1}{4}} (4-v_0)} \left\{ \frac{1+v}{32} + \frac{1+v}{16} \left(\gamma + \ln \frac{\lambda}{8} \right) \right\} - \frac{\bar{\sigma}^{(b)}}{4-v_0} \cdot$$

$$\left\{ 1 - \frac{5+2v+v^2}{(4-v_0)v_0} \frac{\pi\lambda^2}{64} \right\} + O(\lambda^4 \ln \lambda); \qquad \lambda < 2.5 . \qquad (12d)$$

Here again the stress coefficients are only valid for small values of the parameter λ and that for $\lambda > 2.5$ one must consider higher order terms. Fig. 16 gives Duncan's results for $v = 0.32$ and $\bar{\sigma}^{(b)} = 0$. Notice that for small λ's $(\lambda < 2.5)$ the stress coefficients given by (11d) and (12d) and Duncan's results are identical.

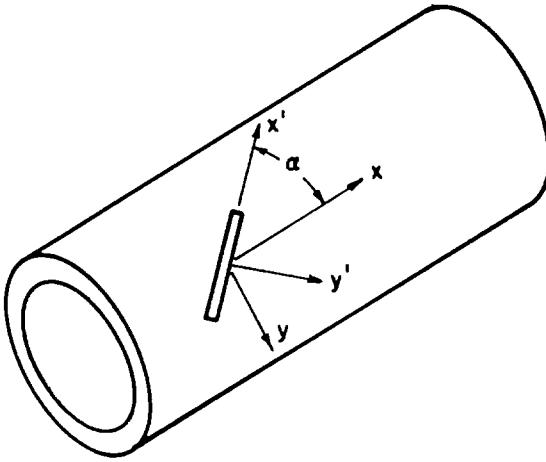(iii) *for an arbitrary orientation crack*★ (see Fig. 17)

Figure 17. Coordinates of an arbitrarily oriented crack in a cylindrical shell.

$$P_{c,\alpha}^{(e)} = \bar{\sigma}^{(e)} \left\{ 1 + \frac{(5 \cos^2 \alpha + \sin^2 \alpha)\pi\lambda^2}{64} \right\} \pm \bar{\tau}^{(e)} \left\{ 1 + 5^{\frac{1}{4}} \frac{\pi\lambda^2}{64} \sin 2\alpha \right\}$$

$$+ \bar{\sigma}^{(b)} \frac{\lambda^2 (1-v^2)}{3^{\frac{1}{4}} (4-v_0)} \left\{ \left[\frac{42-37v_0}{96v_0} + \frac{6-5v_0}{16v_0} \left(\gamma + \ln \frac{\lambda \cos \alpha}{8} \right) \right] \cos^2 \alpha \right.$$

$$\left. + \left[\frac{1+v}{32v_0} + \frac{1+v}{16v_0} \left(\gamma + \ln \frac{\lambda \sin \alpha}{8} \right) \right] \sin^2 \alpha \right\}$$

$$\pm \bar{\tau}^{(b)} \cdot \frac{\lambda^2 (1-v^2)^{\frac{1}{4}}}{3^{\frac{1}{4}} (4-v_0)} \left\{ \frac{42-37v_0}{96v_0} + \frac{6-5v_0}{16v_0} \left(\gamma + \ln \frac{\lambda \cos \alpha}{8} \right) \right\}^{\frac{1}{4}} \times$$

$$\times \cdot \left\{ \frac{(1+v)}{32v_0} + \frac{(1+v)}{16v_0} \left(\gamma + \ln \frac{\lambda \sin \alpha}{8} \right) \right\}^{\frac{1}{4}} \sin 2\alpha + O(\lambda^4 \ln \lambda); \qquad \lambda < 1 \qquad (11e)$$

★ Approximate stress intensity factors; for derivation see appendix. It should be emphasized here that the angular distribution associated with $\bar{\tau}^{(e)}$ and $\bar{\tau}^{(b)}$ is not that given by eqns. (5)–(10), but similar. See reference [3b] for the exact solution of the antisymmetric problem in a spherical shell.

$$P_{c,\alpha}^{(b)} = -\bar{\sigma}^{(e)} \frac{\lambda^2(3^{\frac{1}{2}})}{(1-v^2)^{\frac{1}{2}}(4-v_0)} \left\{ \left[\frac{42-37v_0}{96} + \frac{6-5v_0}{16}\left(\gamma + \ln\frac{\lambda\cos\alpha}{8}\right) \right] \cos^2\alpha \right.$$

$$\left. + \left[\frac{1+v}{32} + \frac{1+v}{16}\left(\gamma + \ln\frac{\lambda\sin\alpha}{8}\right) \right] \sin^2\alpha \right\}$$

$$+ \bar{\tau}^{(e)} \frac{\lambda^2(3^{\frac{1}{2}})}{(1-v^2)^{\frac{1}{2}}(4-v_0)} \left\{ \left[\frac{42-37v_0}{96} + \frac{6-5v_0}{16}\left(\gamma + \ln\frac{\lambda\cos\alpha}{8}\right) \right]^{\frac{1}{2}} \times \right.$$

$$\left. \left[\frac{1+v}{32} + \frac{1+v}{16}\left(\gamma + \ln\frac{\lambda\sin\alpha}{8}\right) \right]^{\frac{1}{2}} \right\} \sin 2\alpha$$

$$- \frac{\bar{\sigma}^{(b)}}{4-v_0} \left\{ 1 - \frac{(1+2v+5v^2)\cos^2\alpha + (5+2v+v^2)\sin^2\alpha}{(4-v_0)v_0} \frac{\pi\lambda^2}{64} \right\}$$

$$\mp \frac{\bar{\tau}^{(b)}}{4-v_0} \left\{ 1 + \frac{(5v_0^2 - 12v_0 + 8)^{\frac{1}{2}}(v^2+2v+5)^{\frac{1}{2}}}{(4-v_0)v_0} \frac{\pi\lambda^2}{64} \sin 2\alpha \right\} + O(\lambda^4 \ln \lambda); \lambda < 1 \quad (12e)$$

or the alternate numerical form valid only for $\bar{\sigma}^{(b)} = 0$, $v = \frac{1}{3}$, and $\lambda \leq 8$

$$P_{c,\alpha}^{(e)} = \bar{\sigma}^{(e)} \left\{ 1 + (\tilde{P}_{c,a}^{(e)} - 1)|_{\lambda = \lambda\cos\alpha} + (\tilde{P}_{c,p}^{(e)} - 1)|_{\lambda = \lambda\sin\alpha} \right\}$$

$$\pm \bar{\tau}^{(e)} \left\{ 1 + (\tilde{P}_{c,a}^{(e)}|_{\lambda = \lambda\cos\alpha} - 1)^{\frac{1}{2}} \ (\tilde{P}_{c,p}^{(e)}|_{\lambda = \lambda\sin\alpha} - 1)^{\frac{1}{2}} \right\} \quad (13e)$$

$$\tilde{P}_{c,\alpha}^{(b)} = -\bar{\sigma}^{(e)} \left\{ \tilde{P}_{c,a}^{(b)}|_{\lambda = \lambda\cos\alpha} + \tilde{P}_{c,p}^{(b)}|_{\lambda = \lambda\sin\alpha} \right\} \mp \bar{\tau}^{(e)} \left\{ (\tilde{P}_{c,a}^{(b)}|_{\lambda = \lambda\cos\alpha})^{\frac{1}{2}} (\tilde{P}_{c,p}^{(b)}|_{\lambda = \lambda\sin\alpha})^{\frac{1}{2}} \right\} \quad (14e)$$

where $\tilde{P}^{()} \equiv \dfrac{P^{()}}{\bar{\sigma}^{(e)}}$.

4. Approximate stress factors for other shell geometries

If one chooses the coordinate axes x and y such that they are parallel to the principal radii of curvature*, then

$$\frac{\partial^2 w_0}{\partial x \, \partial y} = 0 \; ; \quad \frac{\partial^2 w_0}{\partial x^2} = \frac{1}{R_x} \; ; \quad \frac{\partial^2 w_0}{\partial y^2} = \frac{1}{R_y} , \quad (3f)$$

with R_x and R_y being the principal radii of curvatures in the x and y directions respectively. Substituting (3f) into (1) and (2) one finds

$$Eh\left[\frac{1}{R_y} \frac{\partial^2 w}{\partial x^2} + \frac{1}{R_x} \frac{\partial^2 w}{\partial y^2} \right] + \nabla^4 F = 0 \quad (1f)$$

$$\nabla^4 w - \frac{1}{D}\left[\frac{1}{R_y} \frac{\partial^2 F}{\partial x^2} + \frac{1}{R_x} \frac{\partial^2 F}{\partial y^2} \right] = -\frac{q}{D} . \quad (2f)$$

However, inasmuch as the complementary solution or perturbed solution presents contributions only in the immediate vicinity of the crack tip, one may consider—at least locally—the principal radii of curvatures constant. Thus assuming that the crack is parallel to one of the principal axes, say along the x-axis, one may hypothesize that the stress coefficients depend primarily on the curvatures that one observes as he travels parallel and perpendicular to the crack. Consequently, one may estimate the stress coefficients by a proper superposition of the results of an axial and a peripheral crack in a cylindrical shell. In particular, for $\bar{\sigma}^{(b)} = 0$

$$P^{(e)} \approx \bar{\sigma}^{(e)} \left\{ 1 + \frac{\pi\lambda_x^2}{64} + \frac{5\pi\lambda_y^2}{64} \right\} \quad (11f)$$

---

* In a more general case, when they are not parallel, equations (1f) and (2f) will contain additional terms of the form $(\partial^2 w/\partial x \, \partial y)$ and $(\partial^2 F/\partial x \, \partial y)$ For the angular distribution of this case, see footnote on page 7.

$$P^{(b)} \approx -\bar{\sigma}^{(e)} \frac{3^{\ddagger}}{(1-v^2)^{\ddagger}(4-v_0)} \left\{ \frac{42-37v_0}{96} \lambda_x + \frac{6-5v_0}{16} \lambda_y^2 \left(\gamma + \ln \frac{\lambda_y}{8} \right) \right.$$

$$\left. + \frac{1+v}{32} \lambda_x^2 + \frac{1+v}{16} \lambda_x^2 \left(\gamma + \ln \frac{\lambda_x}{8} \right) \right\} + O(\lambda \ln \lambda); \qquad \lambda < 1 \qquad (12\text{f})$$

or the alternate numerical form valid for $v = \frac{1}{3}$ and $\lambda \leqq 8$

$$P^{(e)} \approx \quad \bar{\sigma}^{(e)} \left\{ 1 + (P_{c,a}^{(e)} - 1)|_{\lambda=\lambda_y} + (P_{c,p}^{(e)} - 1)|_{\lambda=\lambda_x} \right\} \tag{13f}$$

$$P^{(b)} \approx -\bar{\sigma}^{(e)} \left\{ P_{c,a}^{(b)}|_{\lambda=\lambda_y} + P_{c,p}^{(b)}|_{\lambda=\lambda_x} \right\}. \tag{14f}$$

In order to check the validity of such a superposition we will consider as our first example★ a spherical cap the stress coefficient for which we know exactly.

Example 1: Sphere. For this shell the curvature is constant in all directions therefore, in view of equations (11f) and (12f), one has

$$P_s^{(e)} \approx \bar{\sigma}^{(e)} \left\{ 1 + \frac{\pi \lambda^2}{64} + \frac{5\pi \lambda^2}{64} \right\} = \bar{\sigma}^{(e)} \left\{ 1 + \frac{3\pi \lambda^2}{32} \right\}; \qquad \lambda < 1$$

which is identical to the exact (see eqn. 11a). Similarly

$$P_s^{(b)} \approx -\bar{\sigma}^{(e)} \frac{(3^{\ddagger})\lambda^2}{(1-v^2)^{\ddagger}(4-v_0)} \left\{ \frac{42-37v_0}{96} + \frac{6-5v_0}{16} \left(\gamma + \ln \frac{\lambda}{8} \right) + \frac{1+v}{32} + \frac{1+v}{16} \left(\gamma + \ln \frac{\lambda}{8} \right) \right\}$$

$$= -\bar{\sigma}^{(e)} \frac{(3^{\ddagger})\lambda^2}{(1-v^2)^{\ddagger}(4-v_0)} \left\{ \frac{-0.1+5v}{32} + \frac{1+3v}{8} \left(\gamma + \ln \frac{\lambda}{4} \right) \right\}; \qquad \lambda < 1$$

which agrees fairly well with (12a). One may conclude, therefore, that such a hypothesis may not be unreasonable.
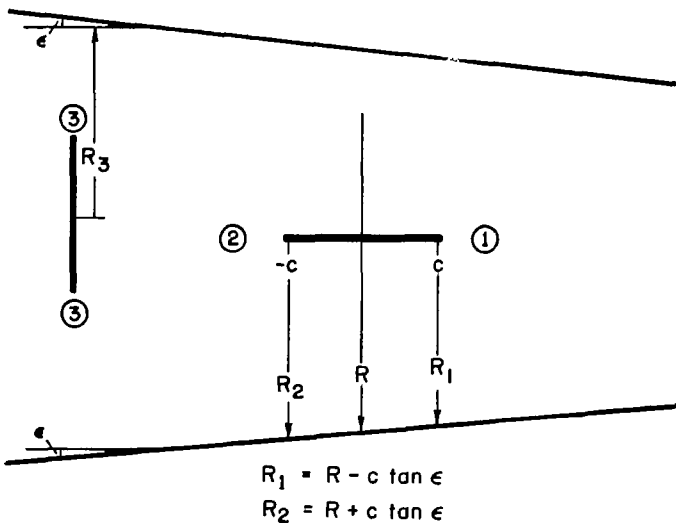

Figure 8. Conical singular shell.

Example 2: Circular conical shell (see Fig. 18). In this case, one curvature is infinite the other finite, therefore,

★ In the following examples, we have assumed $\bar{\sigma}^{(b)} = 0$.

(i) *for an axial crack*:

$$P_{①}^{(e)} \approx \bar{\sigma}^{(e)} \left\{ 1 + \frac{5\pi}{64} \lambda_1^2 \right\} ; \qquad \lambda_1 < 1$$

$$P_{②}^{(e)} \approx \bar{\sigma}^{(e)} \left\{ 1 + \frac{5\pi}{64} \lambda_2^2 \right\} ; \qquad \lambda_2 < 1$$

(ii) *for a peripheral crack*

$$P_{③}^{(e)} \approx \bar{\sigma}^{(e)} \left\{ 1 + \frac{\pi}{64} \lambda_3^2 \right\} ; \qquad \lambda_3 < 1$$

where

$$\lambda_1^2 \equiv \{12(1-\nu^2)\}^{\frac{1}{2}} \frac{c^2}{(R - c\tan\varepsilon)h}$$

$$\lambda_2^2 \equiv \{12(1-\nu^2)\}^{\frac{1}{2}} \frac{c^2}{(R + c\tan\varepsilon)h}$$

$$\lambda_3^2 \equiv \{12(1-\nu^2)\}^{\frac{1}{2}} \frac{c^2}{R_3 h}$$

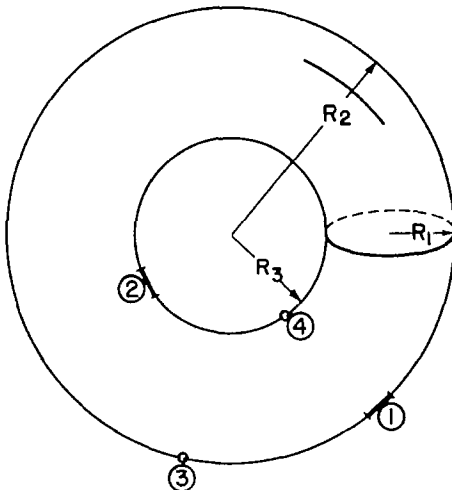*Example* 3 : Toroidal shell (see Fig. 19). For an axial crack in the outer surface

Figure 19. Toroidal shell.

$$P_{①}^{(e)} \approx \bar{\sigma}^{(e)} \left\{ 1 + \frac{5\pi}{64} \lambda_1^2 + \frac{\pi}{64} \lambda_2^2 \right\} ; \qquad \lambda_{1,2} < 1$$

for an axial crack in the inner surface

$$P_{②}^{(e)} \approx \bar{\sigma}^{(e)} \left\{ 1 + \frac{5\pi}{64} \lambda_1^2 - \frac{\pi}{64} \lambda_3^2 \right\} ; \qquad \lambda_{1,3} < 1$$

for a peripheral crack in the outer surface

$$P_{③}^{(e)} \approx \bar{\sigma}^{(e)} \left\{ 1 + \frac{5\pi}{64} \lambda_2^2 + \frac{\pi}{64} \lambda_1^2 \right\} ; \qquad \lambda_{1,2} < 1$$

for a peripheral crack in the inner surface

$$P_{④}^{(e)} \approx \bar{\sigma}^{(e)} \left\{ 1 - \frac{5\pi}{64} \lambda_3^2 + \frac{\pi}{64} \lambda_1^2 \right\} ; \qquad \lambda_{1,3} < 1 .$$

Discussion

In view of the above, one may conjecture that in an initially curved sheet, the
  (i) stresses are proportional to $(c/r)^{\frac{1}{2}}$
 (ii) stresses have the same angular distribution as that of a flat plate
(iii) stress intensity factors are functions of the shell geometry and in the limit we recover the flat plate
 (iv) stresses include interaction terms for bending and stretching.
  A typical term is of the form

$$\frac{\sigma_{\text{shell}}}{\sigma_{\text{plate}}} \approx 1 + \left\{ \frac{a_1}{R_1} + \frac{a_2}{R_2} + \frac{b_1}{R_1} \ln \frac{c}{(R_1 h)^{\frac{1}{2}}} + \frac{b_2}{R_2} \ln \frac{c}{(R_2 h)^{\frac{1}{2}}} \right\} \cdot \frac{c^2}{h} + O\left(\frac{1}{R_1^2}, \frac{1}{R_2^2} \right) \tag{15}$$

where the expression inside the braces is a positive quantity. One concludes, therefore, that the general effect of initial curvature, in reference to that of a flat sheet, is to increase the stresses in the neighborhood of the crack joint and reduce its resistance to fracture initiation.

  It is of some practical value to be able to correlate flat sheet behavior with that of initially curved specimens. In experimental work on brittle fracture, for example, considerable time could be saved since by equation (15) we would expect to predict the response behavior of curved sheets from flat sheet tests.

Particular Solutions

In order to get a better feeling of the stresses in the vicinity of a crack tip, we examine the following two illustrations:

(1) Clamped spherical shell
Consider a clamped segment of a shallow spherical shell of base radius $\bar{R}_0$ and containing at the apex a finite radial crack of length $2c$ (see Fig. 20). The shell is subjected to a uniform internal
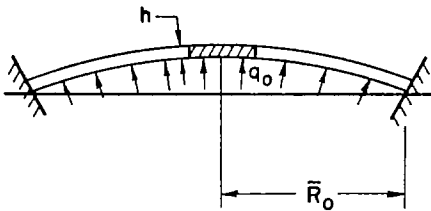

Figure 20. Pressurized spherical cap with fixed ends.

pressure q_0 with radial extension $N_r = (q_0/2)R$, and because it is clamped we require that the displacement and slope vanish at $\bar{R} = \bar{R}_0$. For this problem the residual "applied bending" and "applied stretching" loads at the crack are:* $\bar{\sigma}^{(b)} = 0$ and $\bar{\sigma}_e = q_0 R/2h$. Returning now to the stresses, along the crack prolongation one finds from equations (6), (11a) and (12a) that the normal to the crack stress is

$$\sigma_n(x, 0)|_{v=\frac{1}{2}} \approx \left(\frac{c}{2r} \right)^{\frac{1}{2}} \{ 1 + (0.47 - 0.46 \ln \lambda) \lambda^2 \} (q_0 R/2h) \tag{16a}$$

which for $\lambda = 1$ reduces to:

$$\sigma_n(x, 0) \approx 1.48 \left(\frac{c}{2r} \right)^{\frac{1}{2}} (q_0 R/2h). \tag{16b}$$

* For details, see reference [10].

(2) *Closed cylindrical tank*

Consider a shallow cylindrical shell containing a crack of length $2c$. The shell is subjected to a uniform internal pressure q_0 with an axial extension $N_x = (q_0 R/2)$, $M_y = 0$, far away from the crack. For this problem, if the crack is parallel to the axis of the cylinder, then $\bar{\sigma}^{(b)} = 0$ and $\bar{\sigma}^{(e)} = (q_0 R/h)$. Hence the normal stress along the crack prolongation as found from (6), (11c) and (12c) is:

$$\sigma_n(x, 0)|_{v=\frac{1}{4}} \approx \left(\frac{c}{2r}\right)^{\frac{1}{4}} \{1 + (0.37 - 0.30 \ln \lambda)\lambda^2\}(q_0 R/h) \tag{17a}$$

which for $\lambda = 1$ reduces to:

$$\sigma_n(x, 0) \approx 1.37 \left(\frac{c}{2r}\right)^{\frac{1}{4}} (q_0 R/h) . \tag{17b}$$

If the crack is perpendicular to the axis of the cylinder, then $\bar{\sigma}^{(b)} = 0$ and $\bar{\sigma}^{(e)} = q_0 R/2h$; therefore

$$\sigma_n(x, 0)|_{v=\frac{1}{4}} = \left(\frac{c}{2r}\right)^{\frac{1}{4}} \{1 + (0.20 - 0.15 \ln \lambda)\lambda^2\}(q_0 R/2h) \tag{18a}$$

which for $\lambda = 1$ reduces to:

$$\sigma_n(x, 0) \approx 1.20 \left(\frac{c}{2r}\right)^{\frac{1}{4}} (q_0 R/2h) . \tag{18b}$$

In the event that the crack makes an angle α with the axis of the cylinder, then $\bar{\sigma}^{(b)} = 0$, $\bar{\sigma}^{(e)} = (q_0 R/4h)(3 + \cos 2\alpha)$, $\bar{\tau}^{(e)} = (q_0 R/4h) \sin 2\alpha$. Thus the normal to the crack stress may be derived from equations (6), (11e), and (12e).

Acknowledgement

Appendix

In view of the coordinate transformation (see Fig. 17)

$$x' = y \sin \alpha + x \cos \alpha \tag{19}$$

$$y' = y \cos \alpha - x \sin \alpha .$$

Equations (1c) and (2c) may be written in the form:

$$\frac{Eh}{R}\left[(\cos \alpha)^2 \frac{\partial^2 w}{\partial x^2} - 2(\sin \alpha)(\cos \alpha)\frac{\partial^2 w}{\partial x \partial y} + (\sin \alpha)^2 \frac{\partial^2 w}{\partial y^2}\right] + \nabla^4 F = 0 \tag{20}$$

$$\nabla^4 w - \frac{1}{RD}\left[(\cos \alpha)^2 \frac{\partial^2 F}{\partial x^2} - 2(\cos \alpha)(\sin \alpha)\frac{\partial^2 F}{\partial x \partial y} + (\sin \alpha)^2 \frac{\partial^2 F}{\partial y^2}\right] = -\frac{q}{D} \tag{21}$$

where for simplicity in the above we have dropped the prime notation.

An exact solution of the above equations with the proper boundary conditions is feasible if one uses the same method of solution that the author has developed in previous papers. However, the algebra becomes extremely tedious and time consuming. By studying the governing equations, one notices that by a suitable superposition of the axial and peripheral crack solutions one has the solution of equations (20) and (21), where the cross derivative terms now have been neglected. To account for the cross derivative terms,* we assume that the contribution is equal to the square root of the product of the two $O(\lambda^2)$ correction factors multiplied by the factor $+\sin 2\alpha$ and the appropriate "applied" shear. The results are given by equations (11e) and (12e).

---

* The cross derivative terms correspond to shear.

REFERENCES

[1] P. M. Ogibalov, *Dynamics and Strength of Shells*, translated from Russian, published for NASA and NSF by the Israel Program for Scientific Translations.
[2] K. Marguerre, *Proc. 5th Int. Congr. Appl. Mech.*, 93–101 (1938).
[3] E. S. Folias, *J. Math. Phys.*, 44, 2 (1965) 164–176; ARL 64–23, Aerospace Research Laboratories, United States Air Force, Dayton, Ohio, January 1964.
[4] F. Erdogan and J. Kibler, *Int. J. Frac. Mech.*, 5 3 (September 1969).
[5] E. E. Sechler and M. L. Williams, *The Critical Crack Length in Pressurized Monocoque Cylinders*, Final Report, GALCIT 96, Calif. Inst. Tech., September 1959. See also: M. L. Williams, *Proc. Crack Propagation Symp.*, Cranfield, 1, (1961) 130.
[6] E. S. Folias, Int. J. Frac. Mech., 1, 2 (1965) 104–113; ARL 64–174, Aerospace Research Laboratories, United States Air Force, Dayton, Ohio, October 1964.
[7] E. S. Folias, *Int. J. Frac. Mech.*, 3, 1 (1967) 1–11.
[8] L. G. Copley and J. L. Sanders, *Int. J. Frac. Mech.*, 5, 2 (June 1969).
[9] M. E. Duncan and J. L. Sanders, *Int. J. Frac. Mech.*, 5, 2 (June 1969).
[10] E. S. Folias, *Int. J. Frac. Mech.*, 1, 1 (1965) 20–46.

RÉSUMÉ

Il est procédé à une étude des solutions existantes qui permettent de décrire la distribution des tensions au voisinage de l'extrémité d'une fissure dans une tôle mince présentant une courbure donnée.

L'on discute également une méthode d'estimation approchée des facteurs d'intensité de contrainte dans le cas d'enveloppes à géométrie plus complexe.

ZUSAMMENFASSUNG

Der Verfasser gibt eine Übersicht der Lösungen, welche die Spannungsverteilung in der Umgebung der Spitze eines Risses in einem vorgebogenen Blech beschreiben. Außerdem wird ein Verfahren besprochen, nach dem Spannungsintensitätsfaktoren im Falle komplizierterer geometrischer Formen näherungsweise geschätzt werden können.